Volume 13, Issue 4, Page 66-84, 2024 https://doi.org/10.46810/tdfd.1506516 Research Article

BİNGÖL UNIVERSITY

Türk Doğa ve Fen Dergisi
Turkish Journal of Nature and Science
www.dergipark.gov.tr/tdfd

Design and Mechanical Analyses of Autonomous Mobile Robot with Swerve Driving System

Oğuz MISIR[1*], Melike BEYAZLI [1], Sümeyye ALP [1], Görkem Burak TAŞKIN [1], Zeynep IŞIK[1]

[1]Bursa Teknik Üniversitesi, Mühendislik ve Doğa Bilimleri Fakültesi, Mekatronik Mühendisliği, Bursa, Türkiye
Oğuz MISIR ORCID No: 0000-0002-3785-1795
Melike BEYAZLI ORCID No: 0009-0005-6315-794X
Sümeyye ALP ORCID No: 0009-0006-5922-8706
Görkem Burak TAŞKIN ORCID No: 0009-0004-0483-0404
Zeynep IŞIK ORCID No: 0009-0005-1388-7194

**Corresponding author: oguz.misir@btu.edu.tr*

(Received: 28.06.2024, Accepted: 06.11.2024, Online Publication: 30.12.2024)

Keywords
Finite element analysis, Mobile robot, Autonomous

Abstract: The use of mobile robots has become increasingly prevalent in various sectors, including industry, healthcare, logistics, and services. One of the most crucial attributes of these robots for their intended applications is their capacity to transport payloads. Autonomous mobile vehicles capable of carrying payloads are robots that process data received from their environment through electronic components. They contain and deliver the load to the target location in accordance with the data. This study presents the design of a mobile robot with scissor lift and swerve driving systems. Finite element analysis was employed to investigate the stress and deformation behavior of the designed vehicle under a load. The suitability of the materials used for the design was verified as a result of the analyses. Subsequently, the ability of the real-time driving algorithms to act in possible scenarios is tested in a simulation environment.

Swerve Sürüş Sistemine Sahip Otonom Mobil Robotun Tasarımı ve Mekanik Analizleri

Anahtar Kelimeler:
Sonlu elemanlar analizi, Mobil robot, Otonom

Öz: Mobil robotlar, endüstride, sağlık sektöründe, lojistik sektöründe ve servis hizmetlerinde kullanımıyla giderek artan popülerlik kazanmıştır. Bu robotların kullanım amaçları arasındaki en önemli özellikleri arasında faydalı yük taşıyabilme kabiliyetleridir. Bu maksatla mobil robotun yük taşıma kabiliyetinin kazandırılmasında tasarım ve donanım önem kazanmaktadır. Bu çalışmada, makaslı kaldıraç sistemine sahip olan ve "swerve" sürüş sistemiyle hareket eden mobil robotun tasarımı sunulmaktadır. Tasarlanan aracın yük altındaki gerilim ve deformasyon değişimlerini incelemek için sonlu elemanlar kullanılmıştır. Analizler sonucunda kullanılan malzemelerin tasarıma uygunluğu kontrol edilmiştir. Yapısal analizi tamamlanan aracın gerçek zamanlı sürüş algoritmalarının olası senaryolar karşısındaki hareket kabiliyeti simülasyon ortamında test edilmiştir.

1. INTRODUCTION

In a world characterized by constant change, the capacity to adapt to novel situations and acquire new skills and abilities is essential. Within this context, robots capable of multidirectional movement in time and space are utilized [1]. Robots are technological systems that perceive their environment for specific purposes and generate motion plans by evaluating the information they obtain [2]. They have a wide range of applications, including industrial

manufacturing, healthcare, space exploration, and domestic use [3]. Consequently, robotics has become a pervasive feature of the contemporary world, including roles directly oriented towards humans, and is employed in numerous contexts. The human need for technological solutions, which has consistently influenced the evolution of technology, has led to the development of mobile robots, as stationary robots are no longer sufficient.

Autonomous robotic systems are increasingly being employed to develop innovative tools to enhance work efficiency and perform multiple operations in diverse environments, as well as a potential countermeasure to the impending issue of labor shortages [4]. Autonomous mobile robots (AMR) are defined as robots that operate in accordance with environmental information obtained by sensors, cameras, artificial intelligence applications, and other means. They autonomously perform assigned tasks [5]. In contrast to many industrial robots, mobile robots are capable of navigating to their task locations without human intervention, possess expansive movement areas, and complete their tasks by reaching the desired location while avoiding obstacles under varying conditions [6]. Mobile robots are increasingly utilized in numerous industrial and specialized applications. They can be designed according to the specific requirements of their intended use. Mobile robots, which are equipped with various components for different purposes and controlled by diverse software algorithms, are capable of detecting environmental data such as lines, light, and sound autonomously and moving automatically. Alternatively, they can be controlled manually with the assistance of a user interface. The motion mechanisms of mobile robots represent a crucial aspect. Although the motion mechanisms in the vehicle affect numerous parameters, the selection of an appropriate wheel for the vehicle and the creation of wheel configurations on the chassis result in the vehicle being used with high efficiency [7]. Mobile robots are categorized into three types according to their motion mechanism: wheeled, tracked, and legged systems.

The wheel is the most commonly used motion mechanism in mobile robots. Wheeled robots have been the most prevalent locomotion mechanism due to their simple structure, high acceleration, and ease of control. One of the most widely used wheeled mobile robots in industry is the autonomous mobile robot for load handling [8].

The designs of robots used for load-carrying vary according to the manner in which they lift and carry the load. In this context, the weight and dimensions of the load to be transported are the most critical parameters in the system design. Mechanical tests of prototypes made in this field provide great convenience for the design process, cost, and optimization through simulation programs. Consequently, software programs are capable of conducting analyses of interdisciplinary studies, such as mechanics, structural analysis, computational fluid dynamics, and heat transfer, employing the finite element method [5].

The Finite Element Method (FEM) is a numerical analysis technique used to solve complex engineering problems and predict the behavior of a structure or system when subjected to physical effects. This method is based on the principle of dividing the design into small finite elements and analytically examining each element [9]. FEM allows for the identification of potential weak points in the design, optimization of material usage, and verification of safety factors. Additionally, it simulates the system's stress, deformation, and other mechanical properties before producing physical prototypes, thereby helping to reduce costs and accelerate the design process. Consequently, it ensures that the design can operate reliably even under the most challenging conditions, thus preventing potential design errors.

This paper presents the design of an autonomous mobile robot with load-carrying capability developed in a Computer-Aided Design (CAD) environment. The mechanical system of the designed mobile robot was analyzed using the Finite Element Analysis (FEA) method to assess total deformation and stress. Furthermore, the wheel driving capability of the vehicle and mechanism of the scissor system were tested in a simulation environment. In the rest of the paper, Section 2 describes the system, programs used, general control mechanism, structural characteristics of the designed vehicle, and types of mechanical analysis used. Section 3 presents the analysis set-up and test results. Section 4 discusses the overall conclusion of the paper.

1.1 Related Works

In this section, within the scope of our study on AMRs, we review the literature on the utilization of AMRs in the industrial and social domains, mechanical analysis, and simulations of driving systems. The keywords “AMR,” “ANSYS,” “Driving Systems,” and “Simulation” were employed in the literature search. A summary of the pertinent studies identified using these keywords is presented in Table 1. AMRs utilized for material handling and storage in the industry can be readily integrated with various mapping techniques, providing a significant advantage for transportation operations.

AMRs are employed not only in industrial logistics but also in numerous areas for societal benefits. AMRs have recently become prevalent, particularly in the healthcare sector, where they have been effectively utilized for the transportation of medicines and food within hospitals. Baskoro et al. [10], in their study titled “An Autonomous Mobile Robot Platform for Medical Purpose”, asserted that the highly maneuverable AMR named ROM20 can be utilized in various applications such as disinfectant mist spraying and food distribution heating in a hospital environment. This study demonstrates the functionality of AMRs in the healthcare field. In another study by Yan et al. [11] posited that AMRs provide significant advantages in material-handling operations in industrial applications. They also noted that AMRs face flexibility challenges in path alterations but overcome this issue by employing Simultaneous Localization and Mapping (SLAM) techniques.

Recent advancements in drive mechanisms for autonomous robots with high maneuverability have led to substantial progress. The work of Dhelika et al. [12] serves as an exemplar, wherein a motorized hospital bed utilizing a swerve drive mechanism was developed to provide holonomic mobility in healthcare environments. The simplicity and cost-effectiveness of the swerve drive system facilitate its integration into existing systems with minimal modifications. Additionally, the work by Ziqi et al. [13] presents significant research on drive mechanisms and mobility systems for autonomous mobile robots. This study thoroughly examines the advantages and challenges of swerve drive systems, proposing novel methods for enhancing maneuverability and mechanical durability. The research strengthens the scientific foundation of the swerve drive system utilized in our vehicle and directly relates to previous studies on drive mechanisms.

The mechanical design and analysis of autonomous mobile robots have been extensively studied using simulation tools such as Ansys, which provides robust capabilities for structural and dynamic evaluations. Demir et al. [14] conducted static and dynamic analyses of a mobile transportation robot with mecanum wheels, utilizing Ansys Workbench to assess the robot's structural integrity under a maximum load of 300 N. The study calculated critical parameters such as maximum stress and deformation to validate the design under extreme operating conditions. In another study, Prabhakaran et al. [15] focused on a mobile robot designed for material handling, analyzing the structural behavior of the robot's chassis under a 300 N payload. The researchers utilized Ansys to simulate and validate the mechanical integrity of the chassis, ensuring the design could withstand the operational stresses, with maximum stress values of 35.99 MPa and deformation calculated at 0.000248 m.

Simulations of autonomous mobile robots and robotic systems are extensively employed to enhance the accuracy and efficiency of real-time applications. Koca et al. [16] simulated a mobile tank-driving robot in ROS and Gazebo environment. In this study, the physical and inertial properties of the robot were defined, and the motion and control of the robot were simulated. The simulations have made significant contributions in terms of identifying the challenges that mobile robots may encounter in real environments. Specifically, modeling and simulation of tank driving systems increase the reliability of real-time applications and facilitate the development of these systems. Ağralı et al. [17] simulated robot arms with the V-REP (CoppeliaSim) simulator. In the study, MATLAB and V-REP were synchronized to control the robot arm with a PID controller, and trajectory tracking and torque control were simulated with forward and inverse kinematic methods. This approach has been employed to ensure the accurate operation of robot arms, and such simulations are considered an important step towards more precise control of robotic systems.

Table 1. Summary of key studies on AMRs

Study	Focus Area	Techniques Used	Key Findings
Baskoro et al. (2020) [10]	Use of AMRs in healthcare	ROM20 AMR in hospital environments	The developed ROM20 AMR was used in various hospital applications such as disinfectant spray and food distribution, demonstrating the functionality of AMRs in healthcare.
Yan et al. (2023) [11]	Material handling in industrial environment	SLAM (Simultaneous Localization and Mapping)	AMRs provide significant advantages in material handling, overcoming flexibility issues in path changes through SLAM techniques.
Dhelika et al. (2021) [12]	Holonomic mobility and drive mechanism	Swerve drive mechanism	The swerve drive mechanism-equipped motorized hospital bed offers simplicity and cost-effectiveness, enabling easy integration into existing systems.
Zhao et al. (2023) [13]	Drive mechanisms and mobility systems in AMRs	Swerve drive system	The study presents new approaches to enhance the maneuverability and mechanical durability of swerve drive systems in AMRs.
Demir et al. (2021) [14]	Mechanical analysis	Static and dynamic analysis with Ansys Workbench	The Mecanum wheeled mobile robot's ability to safely operate under a load of 300 N was analyzed.
Prabhakaran et al. (2021) [15]	Structural durability analysis	SolidWorks and Ansys	The structural design of a mobile robot capable of carrying 30 kg was analyzed to determine maximum stress and deformation values.
Koca et al. (2020) [16]	AMR simulation	Simulation in ROS and Gazebo	A tank-steer mobile robot's physical and control features were successfully simulated for real-time applications.
Ağralı et al.(2020) [17]	Robot arm simulation	MATLAB and V-REP synchronization, PID controller	The robot arm's torque and trajectory control were successfully simulated using inverse and forward kinematic methods.

2. MATERIAL AND METHOD

The AMR development phase is divided into design, mechanical analysis, hardware, software, and simulations. In this study, the CAD program SolidWorks was used for vehicle design. SolidWorks was chosen because of its user-friendly interface, comprehensive range of tools, and robust simulation capabilities. Among CAD programs, SolidWorks facilitates the modeling of complex geometries and rapid visualization of designs. It is also compatible with analytical methods such as the FEM and simulations that incorporate strength analysis [18]. The Ansys software utilized in these simulations directly supports SolidWorks file formats, such as. stl, .sldasm, and parasolid, enabling the seamless transfer of designs to the analysis environment. This approach mitigates the potential issues that may arise during file transfer. Driving simulations were conducted in a CoppeliaSim environment to perform the necessary tests, and the AMR behavior in various scenarios was investigated. Figure 1 shows the design stages of the mobile robot with payload-carrying capability.

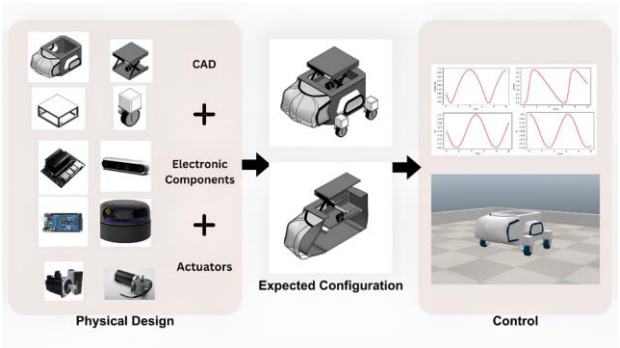

Figure 1. Design stages of a mobile robot with payload-carrying capability

Mechanical analysis is an essential stage in which a model designed with SolidWorks and prepared for analysis must be performed prior to production, particularly when its primary function is load-bearing. Ansys, which is utilized for the mechanical analysis of the vehicle, conducts the analysis using the FEM.

FEM is the process of transforming a finite function into a vector space using numerical methods in the domain of infinite function. [19]. The structure under analysis is divided into a specific number of small parts, termed finite elements, with the objective of mathematically examining the 'behavior' of each part using formulas derived from partial differential equations. The process from a model's real-world state to its discretized state is shown in Figure 2.

Figure 2. The process from a model's real-world state to its discretized state

FEA encompasses specific components such as thermal, electromagnetic, fluid, and structural operating environments. This analytical method provides a detailed visualization of structural deformation and torsion, while simultaneously illustrating the distribution of stresses and displacements. In structural simulations, FEA facilitates the production of stiffness and strength visualizations and contributes to the optimization of weight, materials, and costs. Furthermore, it offers a diverse range of simulation options to regulate the complexity between the modeling and analysis of a system.

In FEA, objects with complex geometries, which are challenging to analyze as a single unit, are subdivided into numerous smaller parts and analyzed separately. These subdivisions are referred to as “mesh”. The mesh constitutes an integral component of the model and requires careful control to obtain the optimal results. Elements comprising small shapes are interconnected by points (nodes) that form the geometry of the model. Figure 3 illustrates the node structure that connects the elements [20].

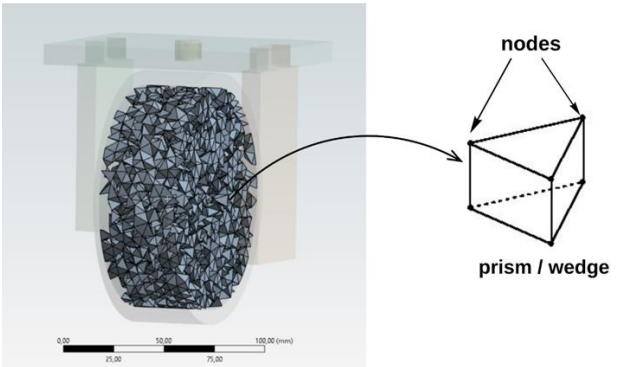

Figure 3. Illustrates the node structure that connects the elements

Mesh quality, element size, and element type are the most critical factors to consider when conducting a mesh analysis. The element size can be reduced in specific regions of the model, which is particularly crucial in critical areas where a high stress or deformation is anticipated. The mesh quality is ensured by through the uniformity of the element shape and optimized size distribution. Optimizing the mesh structure enhances accuracy while maintaining a reasonable solution time. To improve the mesh quality, adjustments are made based on the type and quantity of the elements utilized. Different element types and sizes influence the analysis results [21].

Mesh types are generally categorized as two-dimensional and three-dimensional. Two-dimensional structures are classified as triangular, and quadrilateral meshes. Triangular mesh comprises three-sided elements, and is generally preferred for surface modeling, and is utilized for modeling complex surfaces owing to its flexible structure. A quadrilateral mesh consists of four-sided elements and is often favored to provide more stable results in smooth geometries. Examples of three-dimensional mesh structures include tetrahedral, hexahedral, and wedge meshes. Tetrahedral mesh consists of tetrahedron elements and enables the modeling of complex geometries with high accuracy. Hexahedral mesh comprises hexahedron elements and is suitable for planar structures or regular geometries. Wedge mesh contains prism/wedge elements and is employed in transition zones, complex structures, or when detailed modeling of specific parts is required, which is particularly advantageous in areas that require precise examination.

Selecting appropriate mesh element types for the part reduces the number of elements, thereby decreasing the analysis time and post-analysis processing time. Furthermore, for nonlinear systems and instances in which the arrangement of elements is physically significant, the utilization of hexahedral and quadrilateral

shaped elements is more suitable. Consequently, hex20, tet10, and wed15 were predominantly used in the analysis. The mesh types are also formulated according to the combination of the element types. The mesh types vary based on the arrangement and structure of the elements. Each mesh type presents distinct advantages and disadvantages; therefore, a type that aligns with the requirements of the application should be selected. A structured mesh is preferable for simpler geometries and when expeditious solutions are required, whereas a nonstructured mesh offers a more flexible solution for complex geometries. Hybrid mesh is frequently utilized to balance both accuracy and solution efficiency in complex models. An adaptive mesh is an appropriate method to achieve precise results; however, the processing time and computational cost are higher [21].

The appropriate selection of the mesh structure and type is a critical factor that directly influences the accuracy of the simulation results and the efficiency of the computational process. The determination of which mesh type to employ should be based on consideration of the model geometry and the parameters to be analyzed. Figure 4 shows the Ansys interface of the mesh analyzed part.

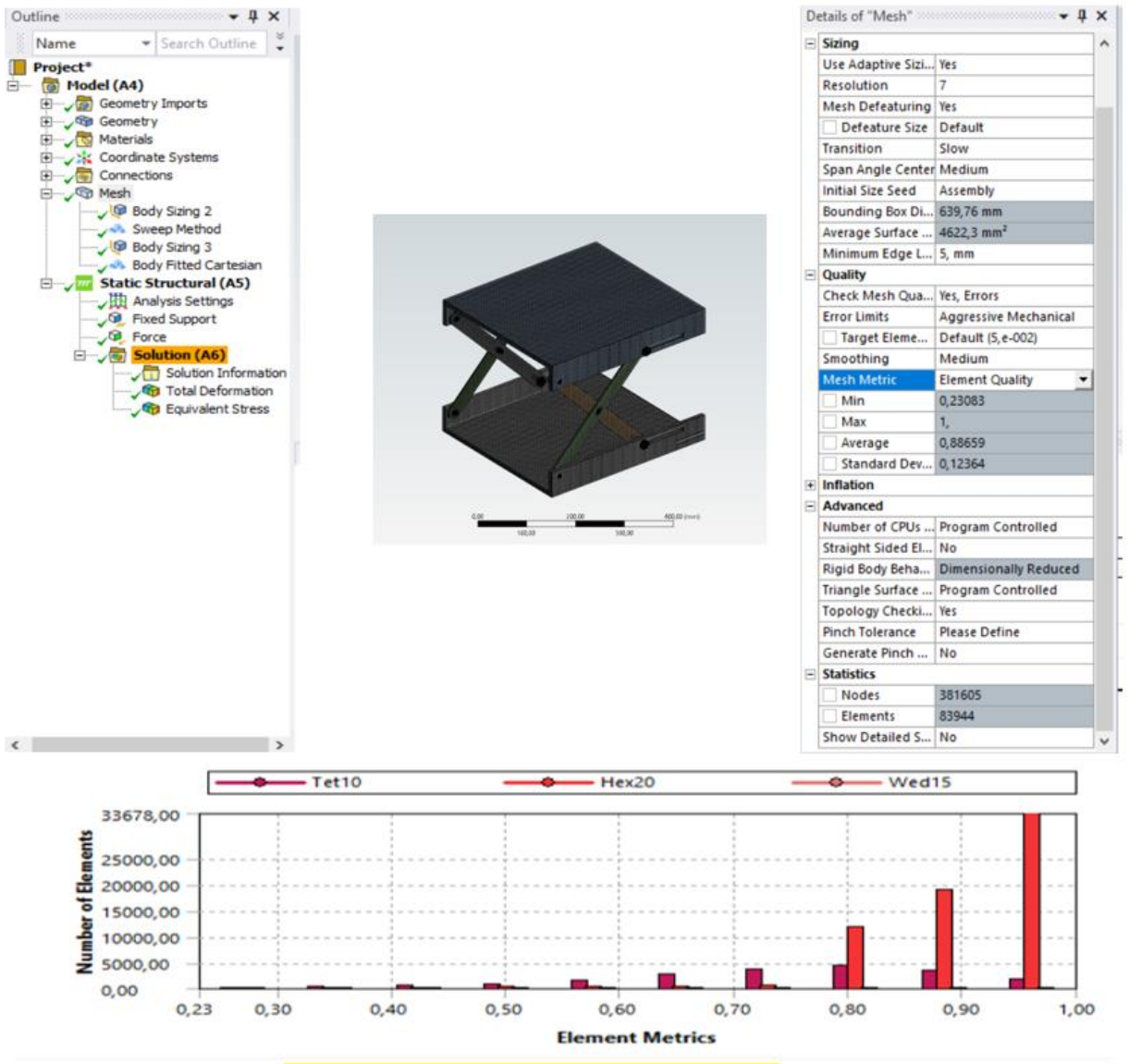

Figure 4. Ansys interface of the mesh analyzed part

Ansys is comprised of various programs for conducting different analyses. In this study, Workbench and Mechanical from the Ansys suite were utilized. Ansys Mechanical, which performs static and dynamic analyses of parts and assemblies in complex structures as well as torsion, stress, vibration, and heat transfer analyses, simulates this work and enables the observation of their behavior in real-world conditions [22]. The steps of the FEM in Ansys are schematized in flowchart form in Figure 5.

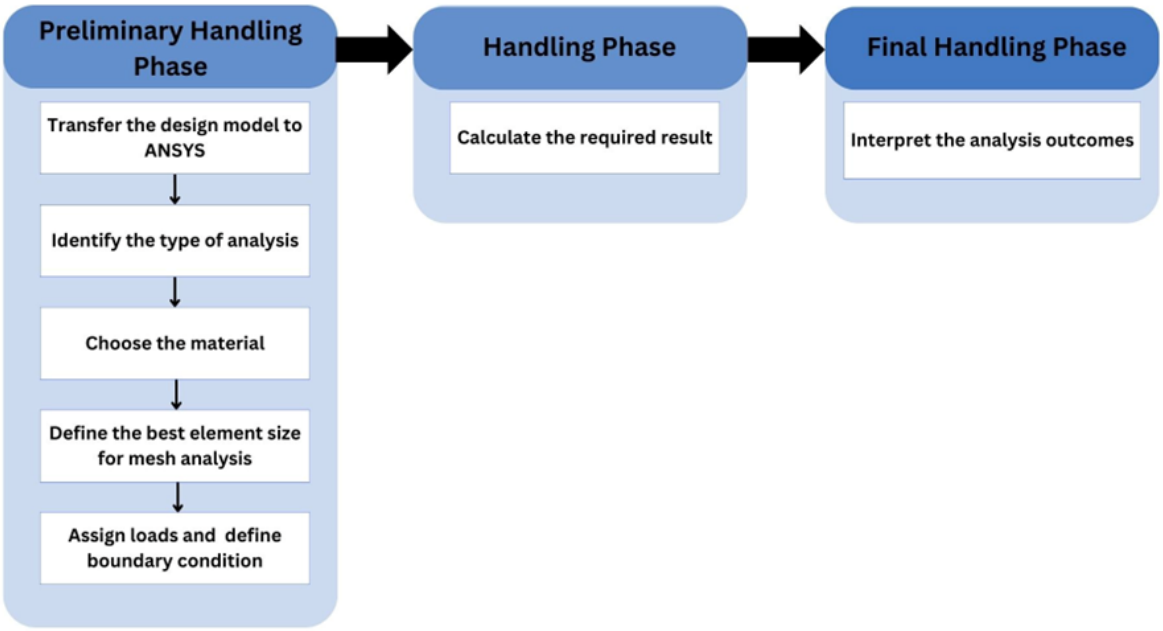

Figure 5. The steps of the FEM in Ansys

In the subsequent phase, simulations are utilized to examine real-time robot system design, modeling, and production, encompassing computer, electronics, mechanics, and control systems, among other interdisciplinary aspects. This process evaluates the performance of the model in the design verification stage prior to initiating production under the specified environmental conditions. Given that simulators are appropriate for conducting necessary tests of a theoretically designed robot or robotic system in a virtual environment, numerous robot simulators such as Gazebo, Webots, and CoppeliaSim have been developed [17]. Among these platforms, CoppeliaSim, which was employed in this study, facilitates the simulation of complex robotic scenarios by creating and manipulating 3D models of robots, sensors, and environments [23]. In the CoppeliaSim environment, the system requires control through code blocks to enable the movement and processing of data received from sensors of the mobile robot. Within the CoppeliaSim simulation environment, Lua Script can be utilized to control the mobile robot's movement via code blocks; alternatively, programming languages such as MATLAB, C/C++, or Python can be employed. Python, a high-level programming language known for its versatility and extensive library support, was selected for the implementation of the motion and deep learning algorithms of the mobile robot [17].
The Spyder integrated development environment (IDE) was employed to develop and manage Python code in conjunction with CoppeliaSim. Spyder provides support for developers and contributes to more effective simulation execution [24].

2.1. Robot Kinematics

Robot kinematics is employed to investigate the motion of robots within a given workspace. By leveraging robot kinematics, the position and orientation of the end effector and the corresponding joint variables can be determined within the robot's operational environment. Robot kinematics is divided into two distinct categories: forward kinematics and inverse kinematics. The forward kinematics of the robot is employed to determine the position of the end effector corresponding to the value of each joint variable, while each joint variable corresponding to the position of the end effector is calculated by inverse kinematics [25].

2.1.1. Wheel kinematics

As the wheel system of the vehicle, as shown in Figure 6, a DC motor was used to rotate the wheel, and a servo motor was used to direct the wheel at certain angles to increase the movement capacity. A total of 8 motors were used in each wheel, one DC motor and one servo motor.

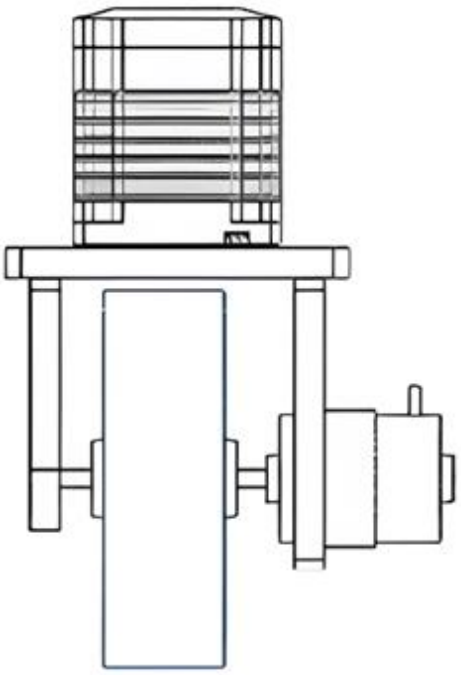

Figure 6. Single wheel structure of the designed vehicle

Vehicle structures with an independent translation and steering module on each wheel are called Wheel Independent Steering or Swerve Drive. Such drive systems are used in weight transportation, agricultural machinery or the Mars Rover. Advantages of the swerve drive system:

- The system provides a high level of mobility. In swerve driving, the direction of movement and orientation are independent, allowing the robot to face forward while moving sideways. Furthermore, the Instantaneous Center of Rotation (ICR) is not fixed in swerve driving, as in ackermann and differential driving. This flexibility allows it to combine linear and rotational movements, which other driving systems cannot do.
- They have wheel structures suitable for payload carrying. Although the degree of freedom is the same as for swerve driving, omni wheels cannot carry the same load due to the lower carrying capacity of the rollers that allow them to move sideways.
- It does not depend on wheel deflections as a multi-wheel differential drive does. This allows the robot to use more motor torque to move forward, consuming less power. While omni and mecanum wheels have movement limitations due to wheel clogging in dust and dirty environments, swerve drive wheels do not have such problems [26]. Figure 7 shows the wheel configurations.

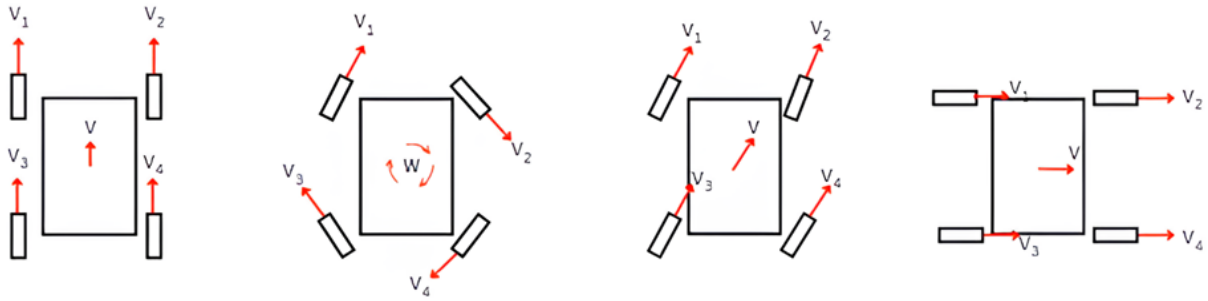

Figure 7. Wheel configurations

In short, in the designed autonomous mobile vehicle, the wheels are controlled independently at different angular speeds. If we consider the single-wheel system, the DC motor performs a rotational motion in the y-axis, which allows the wheel to perform a translational motion in the x-axis. The servomotor adjusts the wheel orientation by rotating in the z-axis. Figure 8 shows the vehicle-wheel axis sets.

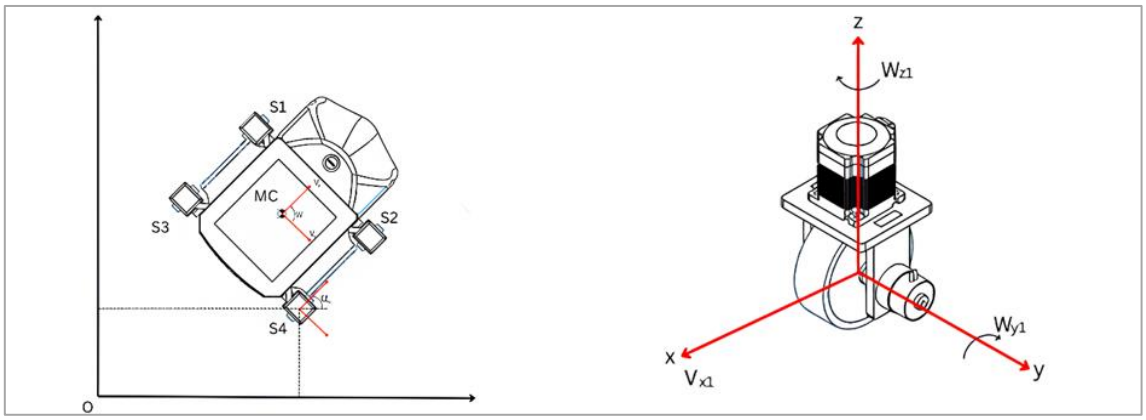

Figure 8. Vehicle-wheel axis sets

The vector sum of the wheel speeds is shown in Equation 1. If the position of the vehicle relative to a fixed set of axes x and y, the direction of our position axis remains constant as the vehicle moves. The position of the single wheel structure relative to the axis of rotation is $\vec{r} = (r_x, r_y, 0)$. When the robot moves with a linear velocity $\vec{v} = (v_x, v_y, 0)$ and an angular $\vec{\omega} = (0,\ 0,\ w_x)$ the linear velocity of the wheel is calculated as in Equation 2 [27].

$$\overrightarrow{v_1} + \overrightarrow{v_2} + \overrightarrow{v_3} + \overrightarrow{v_4} = \vec{V} \quad (1)$$

$$\overrightarrow{V_m} = \vec{V} + \vec{\omega} \times \vec{r} \quad (2)$$

The matrix form of the linear velocity of the wheel is presented in Equation 3. If we assume that the angular velocity of the vehicle is zero, the displacement matrix is as shown in Equation 4. Substituting this equation into Equation 3, Equations 5 and 6 are obtained.

$$\begin{bmatrix} V_{mx} \\ V_{my} \end{bmatrix} = \begin{bmatrix} 1 & 0 & -r_y \\ 0 & 1 & r_x \end{bmatrix} \begin{bmatrix} V_x \\ V_y \\ \omega \end{bmatrix} \quad (3)$$

(r_{0x}, r_{0y}) : The initial position of the wheel in relation to the center of the robot
$\theta(t)$: Heading over time
t : Duration

$$\begin{bmatrix} r_x \\ r_y \end{bmatrix} = \begin{bmatrix} \cos(\omega t) & -\sin(\omega t) \\ \sin(\omega t) & \cos(\omega t) \end{bmatrix} \begin{bmatrix} r_{0x} \\ r_{0y} \end{bmatrix} \quad (4)$$

$$V_{mx}(t) = v_x - \omega \times \left(r_{0x} \times \sin(\omega t) + r_{0y} \times \cos(\omega t)\right) \quad (5)$$

$$V_{my}(t) = v_y + \omega \times \left(r_{0x} \times \cos(\omega t) - r_{0y} \sin(\omega t)\right) \quad (6)$$

$$V_{mx}(t) = v_x - \omega\, x \sqrt{\left({r_{0x}}^2 + {r_{0y}}^2\right)}\, x \cos(\omega t - \tan^{-1}(r_{0x}, r_{0y})) \quad (7)$$

$$V_{my}(t) = v_y + \omega \times \sqrt{\left({r_{0x}}^2 + {r_{0y}}^2\right)} \times \cos(\omega t - \arctan(- r_{0y}, r_{0x}) \quad (8)$$

By applying Equations 7 and 8, the vehicle velocity is calculated sinusoidally according to the origin. The velocity of the wheel:

$$\theta(t) = \arctan\left(v_{my}(t), v_{mx}(t)\right) - \omega t\, , mod\ 2\pi \quad (10)$$

2.1.2. Lift system kinematics

Autonomous mobile robots with payload carrying capability require special payload lifting mechanisms to move payloads from one location to another. These mechanisms can operate both manually and automatically. In general, scissor platforms are the preferred option, as they minimize the footprint of the payload lifting mechanism within the mobile robot and avoid the restriction of its mobility. These platforms are composed of scissors fixed to each other by bearings at the joints, and they offer a high payload capacity and durability.

For the movement of the scissors, the shaft of a servo motor is connected to the cylinder between two opposite scissors. With the rotation of this shaft connected to the servo motor, the scissor bases are shifted back and forth. So the upper platform to which the scissors are connected moves simultaneously on the vertical axis. In line with this movement, the height of the platform is adjusted and the load handling operation takes places. Figure 9 shows mechanism of lift system.

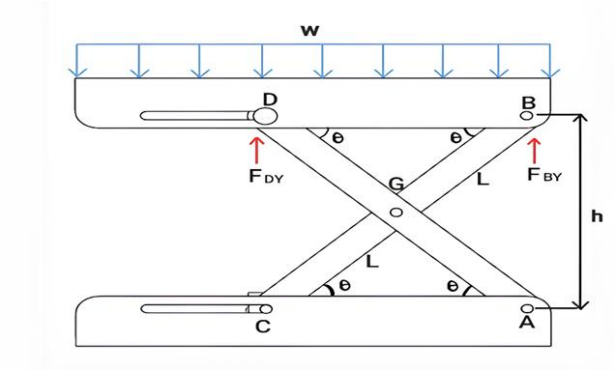

Figure 9. Lift system

W : Distributed load
d_{AC} : Length of AC
L : Length of the scissors
h : Platform height
F_{BY} *and* F_{DY} : Forces applied by the scissors to the platform
L_w : Distance of the distributed load to the moment point

The vertical height of the scissors system to which the upper platform is connected is h, the angle of the scissors with the horizontal is θ and the connections between h and θ are shown in Equation (11-17).

$$L^2 = \left(\frac{h}{2}\right)^2 + \left(\frac{d_{AC}}{2}\right)^2 \quad (11)$$

$$\left(\frac{h}{2}\right)^2 = L^2 - \left(\frac{d_{AC}}{2}\right)^2 \quad (12)$$

$$|\overrightarrow{v_m}(t)| = \sqrt{v_{mx}^2(t) + v_{my}^2(t)} \quad (9)$$

$$\frac{d_{AC}}{2} = \cos\theta \times L \quad (13)$$

$$\left(\frac{h}{2}\right)^2 = L^2 - (cos\theta \times L)^2 \quad (14)$$

$$\left(\frac{h}{2}\right)^2 = L^2(1 - cos\theta^2) = L^2 \times sin\theta^2 \quad (15)$$

$$\sin\theta = \frac{\frac{h}{2}}{L}\ ,\ h = 2 \times L \times \sin\theta \quad (16)$$

$$\frac{d_{AC}}{2} = L \times \cos\theta \quad (17)$$

Instead of point forces, a distributed load is applied to the scissors system. The applied distributed load must be converted into a single singular force in order to substitute it in the moment and force equations. k represents the area of the upper platform where the distributed load is applied, m represents the total mass of the platform and the distributed load. W represents the total force exerted by the upper platform and the distributed load reduced to a singular force. This transformation is shown in Equation 18.

$$W = w \times L \tag{18}$$

During the movement of the scissor system, points A and B remain stationary while points C and D move. Due to this motion, the velocity equations of points C and D are expressed in Equation (19-29) [19].
Velocity equations for point C:

$$V_C = V_G + V_{\frac{C}{G}} \tag{19}$$

$$V_C = V_G + \frac{d}{dt}\left(r_{\frac{C}{G}}\right) \tag{20}$$

$$r_{\frac{C}{G}} = |CG| \times cos\theta \times i + sin\theta \times j \tag{21}$$

$$\frac{d}{dt}\left(r_{\frac{C}{G}}\right) = |CG| \times cos\theta \times \frac{d\theta}{dt} \times i \times sin\theta \times \frac{d\theta}{dt} \times j \tag{22}$$

$$V_{Cx} = \frac{dG}{dt} - |CG| \times \sin\theta \times \frac{d\theta}{dt} \tag{23}$$

$$V_{Cy} = \frac{dG}{dt} - |CG| \times \cos\theta \times \frac{d\theta}{dt} \tag{24}$$

Velocity equations for point D:

$$V_D = V_G + V_{\frac{D}{G}} \tag{25}$$

$$V_D = V_G + \frac{d}{dt}\left(r_{\frac{D}{G}}\right) \tag{26}$$

$$r_{\frac{D}{G}} = |DG| \times \cos\theta \times i + |DG| \times \sin\theta \times j \tag{27}$$

$$V_{Dx} = \frac{dG}{dt} - |DG| \times \sin\theta \times \frac{d\theta}{dt} \tag{28}$$

$$V_{Dy} = \frac{dG}{dt} - |DG| \times \cos\theta \times \frac{d\theta}{dt} \tag{29}$$

The free body diagram of the scissors used in the lifting system is shown in Figure 10. In this diagram, the connection point of the scissors is called G and the connection points between the scissors and the platform are called A, B, C, D.

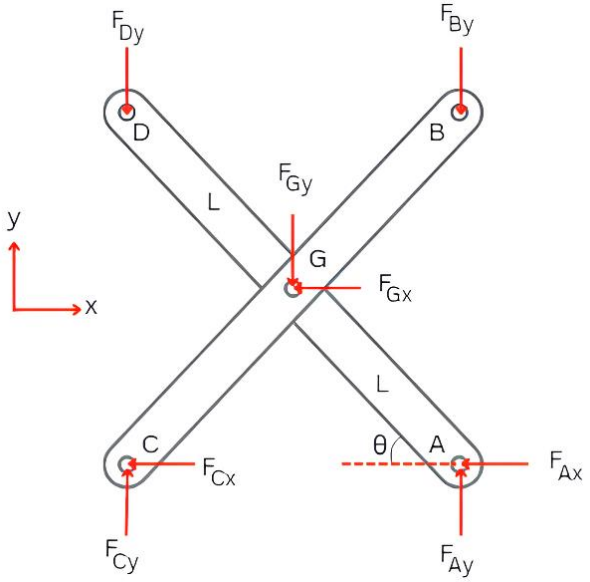

Figure 10. Free body diagram of scissors

The clockwise direction was determined as the direction of rotation of the moment and considered as the positive direction for the whole equation. Then, the total moment and the total force in the x and y axis were calculated for the whole system. These calculations are expressed in Equation below [19].

$$\sum M_D = 0; -W \times |L_w| + 2 \times F_{By} \times |DP| = 0 \tag{30}$$

$$\sum F_y = 0 \;;\; 2F_{Dy} - W + 2F_{By} = 0 \tag{31}$$

$$\sum F_x = 0; \qquad F_{Gx} - F_{Ax} = 0 \tag{32}$$

$$\sum F_y = 0; \qquad -F_{Dy} + F_{Gy} + F_{Ay} = 0 \tag{33}$$

$$\sum M_d = 0; \qquad -F_{By} \times 2 \times \cos\theta - F_{Gy} \times L \times \sin(90-\theta) + F_{Gx} \times L \times \sin\theta \tag{34}$$

$$\sum F_x = 0; \qquad F_{Cx} - F_{Gx} = 0 \tag{35}$$

$$\sum F_y = 0; \qquad -F_{By} - F_{Gy} + F_{Cy} = 0 \tag{36}$$

2.2. Robot Controller

Sensors and simulation environments are often used in robots to obtain the information required for joint handling, such as robot positions, velocities and interaction forces between the load and mobile robots [28]. In order to analyze the motion of the mobile robot in real environment, the URDF file of the vehicle designed in Solidworks is exported to the CoppeliaSim environment. Figure 11 shows the vehicle exported to the CoppeliaSim environment. URDF (United Robotics Description Format) file is a language format written in

accordance with XML (Extensible Markup Language) language structure to describe robots. In this file, "continuous" is used for continuous rotation and "revolute" is used for rotation within a certain angle range.

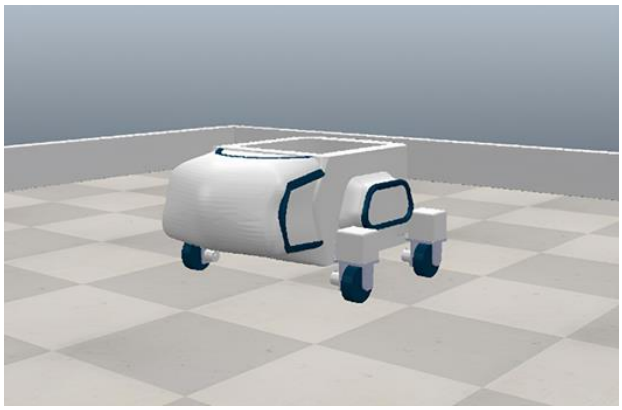

Figure 11. The vehicle exported to CoppeliaSim environment

Python was used to control the parameters of the vehicle exported to the CoppeliaSim environment. To establish a connection between CoppeliaSim and Python language, Spyder IDE, which has an easy and understandable interface and can be easily integrated with CoppeliaSim, was used. In this way, the program is made ready to control the parameters such as velocity, direction and angle of the joint that give the mobile robot the ability to move.

2.3. System design

One of the challenges faced by mobile robots is the problem of localization in an indoor environment. Inaccurate localization can lead to inefficient path planning and inaccurate detection of obstacle locations. Therefore, it is possible to improve the indoor localization of mobile robots by using different sensors. Sensors integrated into the robot include ultrasonic, infrared and laser sensors, as well as LIDAR, depth and stereo vision cameras [29]. Figure 12 shows the system design.

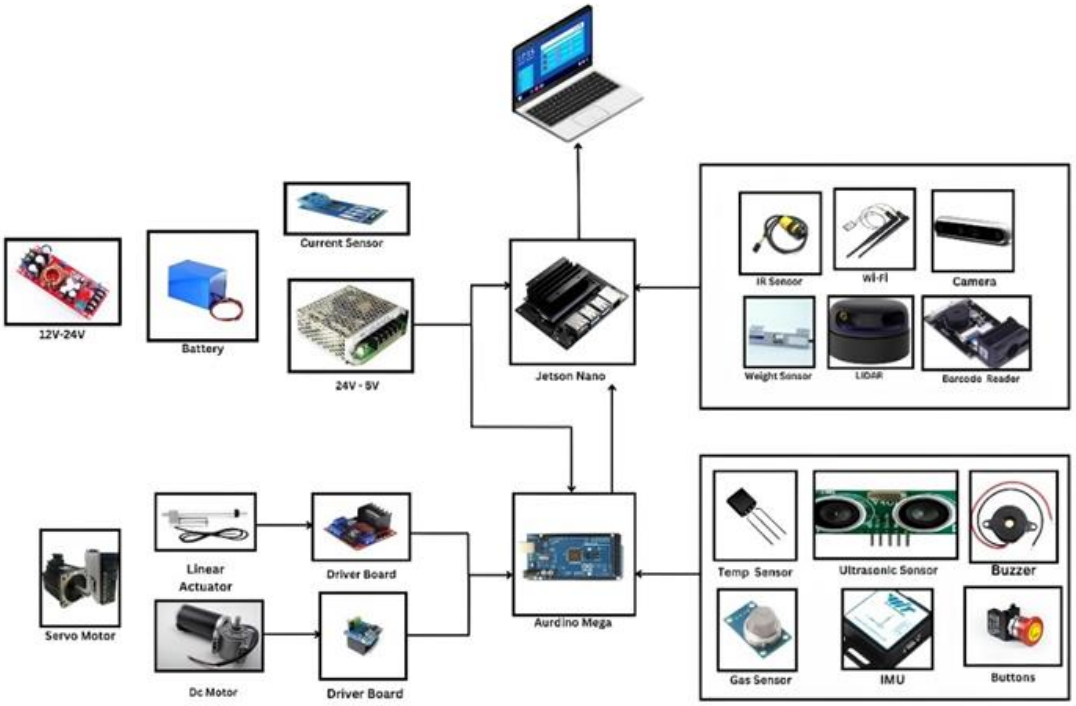

Figure 12. System design

Today, autonomous vehicle technologies are advancing rapidly with the integration of Artificial Intelligence (AI) and deep learning algorithms. These developments require powerful processing capabilities and advanced AI-enabled hardware. NVIDIA Jetson Nano, a platform designed for robotic systems, was used as the main processor board. Jetson Nano manages the processes of collecting and processing data from various sensors in an autonomous vehicle, generating the corresponding control commands, and providing communication between the vehicle and the ground station via a Wi-Fi module. Electronic components connected to the main processor board:

- LIDAR (Laser Imaging Detection and Ranging) is a system that detects the position and distance of objects by sending laser pulses and calculating the return time of signals reflected from objects. In autonomous vehicles, LIDAR sensors continuously scan and map the vehicle's surroundings [30].
- Algorithms that combine camera, depth and image data are used to efficiently perform artificial intelligence tasks such as object recognition, path tracking and mapping.
- The weight sensor is responsible for calculating the weight of an object by measuring the strain on the vehicle. The data obtained from the sensor

is used to determine whether the lift is capable of lifting the load in question.
- Arduino Mega is a coprocessor board used to reduce the processing intensity on the main processor board.

Arduino is an open source physical programming platform that realizes basic input and output applications with peripherals using the processing/wiring language [31].

The Arduino Mega, preferred for its large number of input/output pins and ease of use, sends data from sensors and electronic components to the main processor card. The main processor provides motor control according to the data received from the board. Electronic components connected to the coprocessor board:

- Ultrasonic sensors are detection devices that measure the distance of objects with sound waves. By placing this sensor all around the vehicle, the autonomous vehicle can detect objects and avoid collisions by avoiding objects. This increases the vehicle's ability to maneuver effectively and ensures safe progress.
- IMU is an electronic unit that collects various data such as angular velocity (gyro), acceleration, magnetic field and inclination (inclinometer) in a single sensor. These sensors are needed in areas such as factories where GNSS signals may be insufficient or interrupted [32].
- The motors and driver boards are controlled by Arduino Mega and used to control the motion of DC and servo motors.

2.4. Experimental setup

In the design of AMR, the weight and dimensions of the payload to be transported represent among the most critical factors that directly affect the payload capacity. In order to ensure the safe transportation of the load, it is imperative that the maximum weight does not exceed the capacity of the AMR. The design of the vehicle's transport platform is informed by an understanding of the dimensions of the load. In the process of sizing an AMR the physical characteristics of the area in which it will operate are taken into account. These include the width of roads, narrow passages, and the robot's ability to navigate these environments. Additionally, the design considers the presence of other equipment in the operational environment, such as safety sensors and emergency stop mechanisms. It also ensures that there is sufficient space for batteries and motors, preventing any potential hazards to personnel.

The payload carrying vehicle, which was designed as an original design unlike the current examples, is shown in Figure 14. When designing the vehicle, it was taken as a reference that it can go under a 50x95 cm platform and carry a load of 125 kg. Accordingly, the weight of the vehicle designed in 885×796×464 mm dimensions is approximately 60 kg. According to the dimensions of the vehicle, which is moved with the swerve driving system, the wheel dimensions were determined as 125x40 mm.

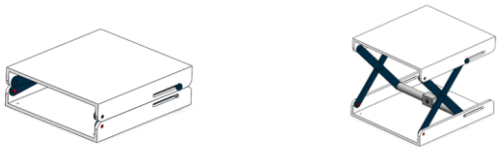

Figure 13. Closed and open state of the scissor system

The scissor system used for load carrying in the mobile robot is 400×360×120 mm in closed state and 400x360x323 in open state and is shown in Figure 13. In addition, the upper platform to which the scissors are connected can be opened to a height of 187 mm from the upper base of the vehicle. The chassis, to which the wheels are attached, and which carries the electronics and the lifting system, has dimensions of 460×500×218 mm. In designing the chassis, several considerations were taken into account, including the ability to safely carry the load and the lifting system, support for the body, dimensions that fit within the body, and sufficient space for electronic components.

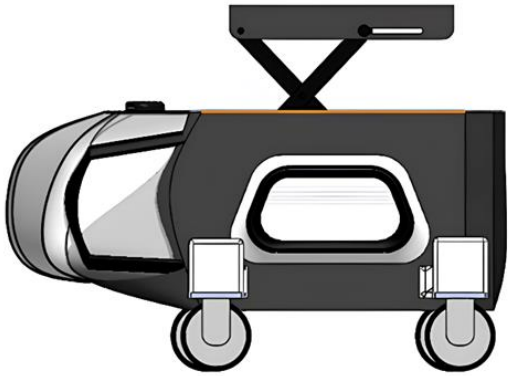

Figure 14. Side view of the designed vehicle

The materials that are scheduled to be utilized in the production of the vehicle are stainless steel and an aluminum alloy. Stainless steel is renowned for its exceptional corrosion and rust resistance in industrial settings, which guarantees the AMR's durability and dependability over an extended period. Furthermore, stainless steel was selected for the scissors, pins, and cylinder due to its superior strength compared to aluminum alloys, which allows for the safe transportation of heavy loads. Aluminum alloy was selected for the body, chassis, wheel joints, and the upper and lower base of the lift due to its lightweight, durable, and easily machinable properties. The reduced weight of aluminum alloys results in decreased energy consumption, which in turn improves the vehicle's driving dynamics and increases maneuverability, thereby extending battery life [33]. The structural properties of the materials used in the mobile vehicle are shown in Table 2.

Table 2. Material information

Properties	Stainless Steel	Aluminum Alloy	Unit
Density	7750	2770	Kg m^{-3}
Young's Modulus	193000	71000	MPa
Poisson Ratio	0.31	0.33	MPa
Shear Modulus	73664	26692	MPa
Yield Strength	207	280	MPa
Tensile Strength	586	310	MPa

The strategic selection of mesh sizes in ANSYS analysis is of great importance in terms of providing the appropriate sensitivity to different regions of the analysed structure. In this study, the smallest mesh size of 3 mm was preferred for critical connection points with high stress concentrations, joints of moving parts and areas with complex geometries. More detailed analyses were performed by using this small mesh size, especially in areas that require precise solutions such as connection points in the lever system and wheel connection areas.

Conversely, the largest mesh size employed in the analysis, 6 mm, was utilised in regions where the load density is more homogenously distributed and does not necessitate high precision. This approach was selected in order to optimise the solution time and reduce the computational load. The largest mesh size was employed for the wheel diameter, while the remaining components were modelled with appropriate mesh sizes between these two sizes. Consequently, different mesh sizes were chosen according to the requirements of each region, resulting in an optimal balance between solution time and accuracy.

The mesh, stress, and deformation analyses of the design were transferred to the static structural module of Ansys for analysis. Initially, a static analysis of the mesh was performed, which examined the real-world behavior of the analyzed parts under load. Based on the analysis, a determination was made regarding the suitability of the materials used in the design.

3. RESULTS

To obtain results approximating real-world conditions from finite element analyses conducted using Ansys, it is essential to carefully examine the values of element quality and skewness derived from the mesh analysis. Element quality can be calculated as the ratio of the volume to the sum of the squares of the edge lengths for 2D elements. In another way, for 3D elements, it is calculated as the square root of the cube of the sum of the squares of the side lengths. Element quality represents a composite quality metric ranging from zero to one. When the parameter value is ‘one’, it indicates an ideal cube or square. When the value is zero, it has a negative volume. [34].

For Mesh, skewness is one of the primary quality measures.Skewness determines the proximity of a face or cell to its ideal (equilateral or equiangular) shape. A skewness value approaching 0 indicates that the element closely approximates its ideal shape (e.g., equilateral shapes for triangular or quadrilateral elements). As the skewness value increases, the elements deviate further from the ideal shape, potentially distorting the analysis results. In Ansys, the skewness value is typically measured on a scale from 0 to 1, with a recommended maximum value of 0.95.Lower skewness values facilitate more accurate analysis results [35].

The results of the analysis show that element quality varies between 0.8 and 1 on average, while skewness is between 0.1 and 0.2. Therefore, it can be concluded that the deformation analysis, which evaluates how much a structure or material changes shape under applied forces and assesses its performance under real-world conditions, and the stress analysis, which determines the internal forces acting within a material and its ability to withstand applied loads, yield results that are close to reality.

The results of the analyses of the body, chassis, wheel mechanism, and lift system are listed in Table (3-6).

3.1. Body

For the outer shell of the vehicle, a body with dimensions of 885×670×355 mm was designed using aluminum alloy, which is a tough material. Figure 16 shows the element metric values of the different mesh types in the car body mesh analysis. It can be seen that element types such as tet10, hex20, wed15, tri3, and quad4 were used. This indicates that a hybrid mesh structure is preferred for representing the complex geometry of the model more accurately.For the outer shell of the vehicle, a body with dimensions of 885×670×355 mm was designed using aluminum alloy, which is a tough material.

The tet10 (tetrahedral) elements used in the analysis are typically preferred for irregular mesh structures and are useful for solving complex geometries. However, they do not provide the same level of accuracy as hexahedral elements do. In contrast, hex20 (hexahedral) elements, which occupy a large space in the model, offer a high solution accuracy and computational efficiency in regular mesh structures. Additionally, wed15 (wedge) elements are used in areas close to the surfaces of the model; these elements are beneficial in regions where triangular-based prismatic structures must align with complex surfaces. The surface elements in the model are represented by tri3 and quad4 elements. tri3 (triangular) elements are preferred for more complex surfaces and irregular areas, while quad4 (quadrilateral) elements are used to convert regular surfaces into a more homogeneous mesh structure [36-37].

In conclusion, the hybrid mesh structure was optimized according to the geometric characteristics by combining both regular and irregular elements. This strategy enhances the solution accuracy while balancing computational costs. In particular, the combined use of hex20 and tet10 elements allows for a denser mesh structure in critical areas, thereby increasing the reliability of the analysis results. The 3D model in Figure 15 illustrates the distribution of these elements over the model, showing the homogeneity of the mesh structure, both on the surface and within the internal structure.

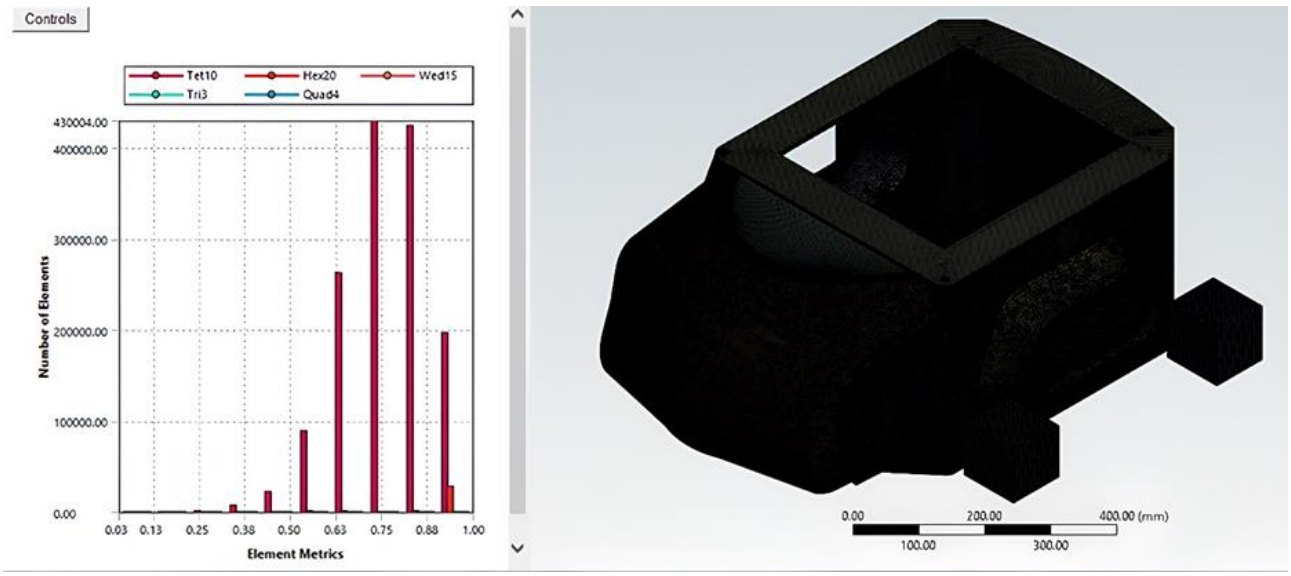

Figure 15. Body mesh analysis

Figure 16 and the data presented in Table 3 were used to evaluate the quality of the mesh structure used in the vehicle body design and the geometric accuracy of its elements. The graph examines various quality metrics of the elements with two particularly significant metrics: element quality and skewness values.

The element quality is a critical factor in determining the analytical accuracy of mesh structures. The average element quality value is 0.78, which is considered acceptable, although the ideal value is closer to 1. A value of 0.78 indicates that most elements possess sufficient quality; however, some elements may exhibit reduced quality. The maximum element quality value is 1, indicating that some elements are of excellent quality, while the minimum quality value of 0.0295 suggests that certain elements have very low quality. Nonetheless, the presence of such low-quality elements in the non-load-bearing sections of the body is unlikely to significantly affect the overall accuracy of the results.

The skewness metric reflects the distortion in the shape of the elements. A low skewness value indicates a better element geometry. The maximum skewness value is 0.99, suggesting that some elements are nearly deformed. Such high skewness values can lead to erroneous deformation and stress analysis. The average skewness value of 0.3 is generally acceptable; however, caution may be necessary in regions where elements exhibit high skewness. The minimum skewness value of 1.3×10^{-10} is nearly zero, indicating that some elements have a very regular shape.
Owing to the complex structure of the body, 1,463,049 elements and 2,798,461 nodes were utilized. This large number of elements signifies a detailed analysis and appropriate representation of the intricate geometry of the body.

These data suggest that, overall, the body mesh structure is sufficient, although improvements could be made in terms of element quality and skewness in certain areas. In particular, during the deformation and stress analyses, elements with high skewness may result in erroneous outcomes. However, considering that these areas do not bear loads, their effect on the overall analysis results is expected to be minimal.

Table 3. Body mesh analysis results

Number of Elements	Number of Nodes	Element Quality	Skewness
1463049	2798461	Max: 1 Avg: 0.78 Min: 0.0295	Max: 0.99 Avg: 0.3 Min:$1.3x10^{-10}$

The effects of the forces on the vehicle's body are evaluated through deformation analyses, as shown in Figure 16, while the stress analyses are presented in Figure 17. The deformation analysis illustrates the deformations that occur under an applied force of 325 N on the body. This analysis is critical for understanding the mechanical stability and durability of the body.

According to the analysis results, the deformation ranged from 0 to 0.55 mm. This is considered a very small deformation range. Given the dimensions of the vehicle body, this amount of deformation can be deemed insignificant. Considering that the body is not a primary load-bearing component and that a durable material such as aluminum alloy is used, it can be stated that this deformation does not pose a safety concern.

In conclusion, the body exhibits good resistance to the applied forces, and the resulting deformation is not significant enough to affect the structural integrity of the vehicle. This indicates that the body was designed safely, with minimal deformation occurring in sections that did not carry loads.

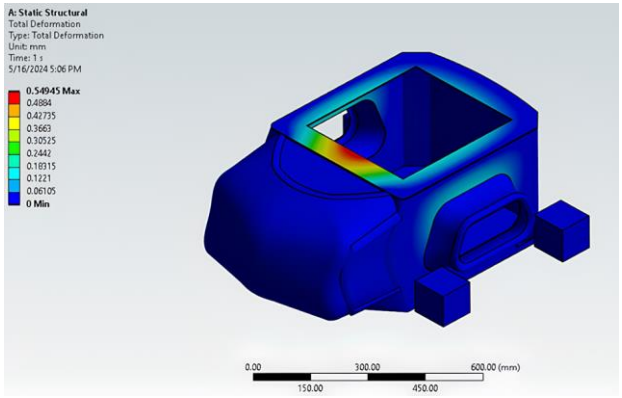

Figure 16. Vehicle body deformation analysis

The stress analysis illustrates the stresses occurring in various regions of the body under the same applied force of 325 N. The stress values range from 0 to 33.6 MPa. Considering the force applied on the body and the mechanical properties of the material, these stress levels are also quite low. Given the mechanical properties of aluminum alloy, these stress levels remain well below the yield limits of the material.

In other words, according to the stress analysis results, the body remained within a safe operating range under the applied forces. No excessive stress occurs in any part of the body, indicating that the design of the body possesses adequate durability against forces and pressures.

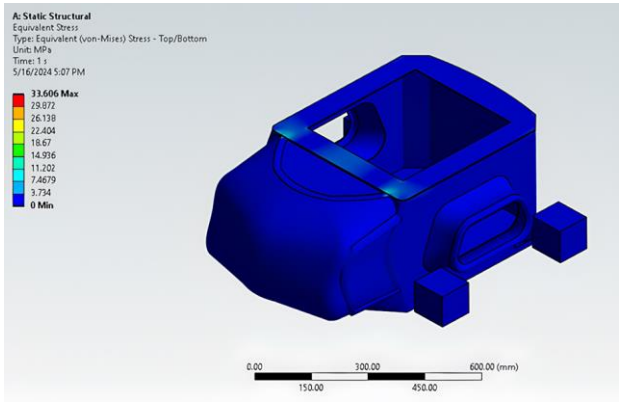

Figure 17. Vehicle body tension analysis

In other words, according to the stress analysis results, the body remained within a safe operating range under the applied forces. No excessive stress occurs in any part of the body, indicating that the design of the body possesses adequate durability against forces and pressures. Both analyses are critical simulations that examine the mechanical properties of the body. The deformation analysis in Figure 16 demonstrates that the body deforms minimally under applied forces. However, the stress analysis in Figure 17 shows that the stresses occurring in different regions of the body remain within a safe range. These results indicate that the design of the vehicle and the materials used are safe against forces and loads and are unlikely to cause issues in the long term.

3.2. Chassis

The chassis has dimensions of 460×500×218 mm and is generally rectangular. Therefore, the chassis, which carries the entire weight and load of the system, is one of the most critical components for autonomous vehicles. Accordingly, the chassis is designed using aluminum alloy, which is both lightweight and durable. The main reason for this is that aluminum increases the carrying capacity while simultaneously reducing the overall weight of the vehicle. In addition, aluminum alloys offer high strength and corrosion resistance, creating long-lasting and durable structures. This is especially critical for autonomous mobile vehicles that operate under harsh environmental conditions.

The mesh structure used in the analysis of the chassis was determined based on the complexity of the geometry and the accuracy of the analysis. Despite the rectangular structure of the chassis, a more flexible and adaptive mesh structure is required in some curved regions and corners. Therefore, the mesh structure shown in Figure 18 was obtained using tetrahedral (tet10) and hexahedral (hex20) elements together for the mesh element, and mesh analysis of this structure was performed. Tetrahedral elements were used in the geometrically complex and angular regions to capture fine details and model complex areas more precisely. On the other hand, hexahedral elements have a more regular structure, especially when used on flat surfaces and rectangular structures, and are preferred on wider and flatter surfaces. The choice of these mesh elements reduced the analysis time and at the same time increased the accuracy of the chassis analysis.

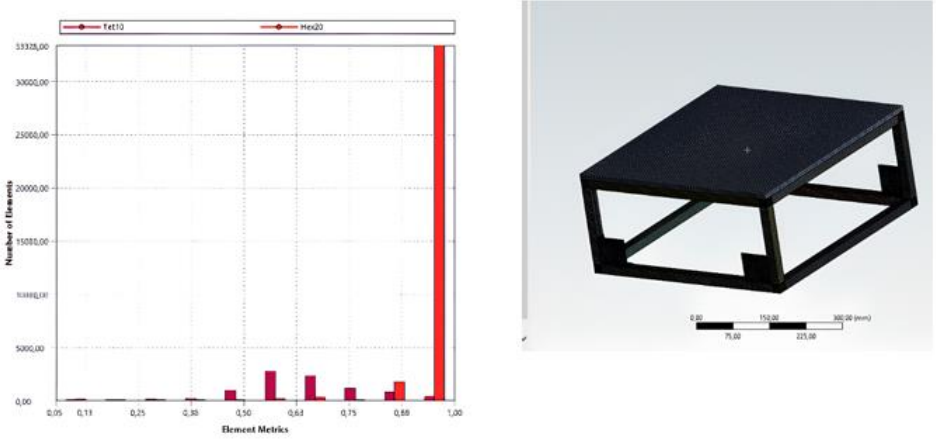

Figure 18. Chassis mesh analysis

The results of the mesh analysis for the chassis are presented in Table 4. According to this table, the chassis contains 43760 elements and 210717 nodes in total. The large number of elements allows the geometry to be modeled in detail and allows better determination of the stress and deformation values at different points of the structure. This is of great importance in the analysis of critical load-bearing structures such as chassis. The maximum element quality calculated in the analysis is 1, and the average quality is 0.89, indicating that the mesh structure is of very high quality. A high element quality improves the accuracy of the analysis results, allowing the stress distributions on the structure to be accurately calculated. On the other hand, skewness, which is another important parameter that evaluates the deformation of the mesh elements, was found to have a maximum value of 0.93 and an average skewness value of 0.1. A low skewness value indicates that the shape of the elements is close to their ideal geometry; thus, the analysis results are reliable.

Table 4. Chassis mesh analysis results

Number of Elements	Number of Nodes	Element Quality	Skewness
43760	210717	Max: 1 Avg: 0.89 Min: 0.0527	Max: 0.93 Avg: 0.1 Min: $1.3x10^{-10}$

The reference force of 1300 N applied to the chassis was calculated according to the lifting capacity of the vehicle and the maximum load it can carry. This force was applied to the chassis, and its durability and deformation capacity were tested. The deformation and stress analyses of the chassis are presented in Figures 19 and 20, respectively. As a result of the analysis, the total deformation values vary between 0 and 0.1878 mm. This deformation range shows that the chassis undergoes minimal deformation under load and, therefore, has sufficient structural strength. In addition, the stress values on the chassis were found between 2.71×10-6 MPa and 35.84 MPa. These values indicate that the material is within the safe operating range by maintaining its elastic limits.

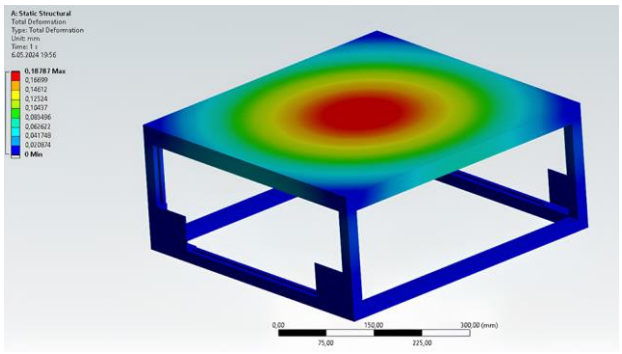

Figure 19. Chassis deformation analysis

Based on the mesh and stress analyses, it is concluded that the chassis design is adequate in terms of both mesh quality and load-carrying capacity. A high-quality mesh structure and low skewness values indicate that the chassis provides reliable analysis results. Considering the stress and deformation results on the chassis, it is concluded that the design is suitable for the production phase.

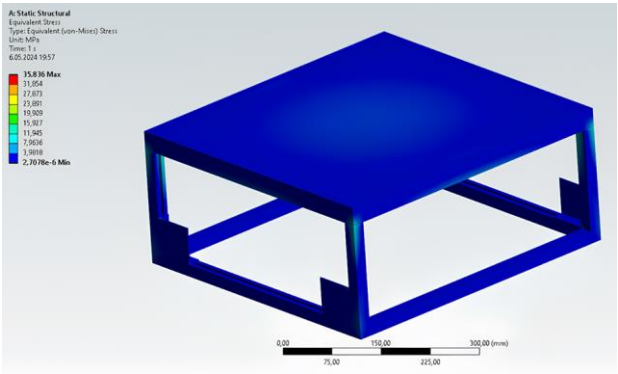

Figure 20. Chassis tension analysis

3.3. Wheel Mechanism

A 125×40 mm drive wheel made of polyurethane material was used in an autonomous mobile vehicle with a Swerve driving system. The polyurethane material wheel, which was selected considering that the autonomous mobile vehicle will be operated in a factory environment, can be under load up to 250 kg; therefore, the wheels were selected as fixed points when performing deformation and stress analysis. The mesh analysis of the aluminum alloy apparatus, which is utilized for the attachment point to the vehicle and the connection of the motors, which are integral to the driving system, to the wheel (the most crucial component), is shown in Figure 21. To enhance the quality of mesh analysis, appropriate element types were selected for the components in question. Cartesian mesh analysis was employed for the rectangular and square parts, whereas the sweep method was used for the cylindrical regions. Additionally, body sizing and face sizing were applied to the remaining parts. Once the requisite mesh types were selected, enhancements were made to the analysis by determining the mesh size according to the overall characteristics of the part.

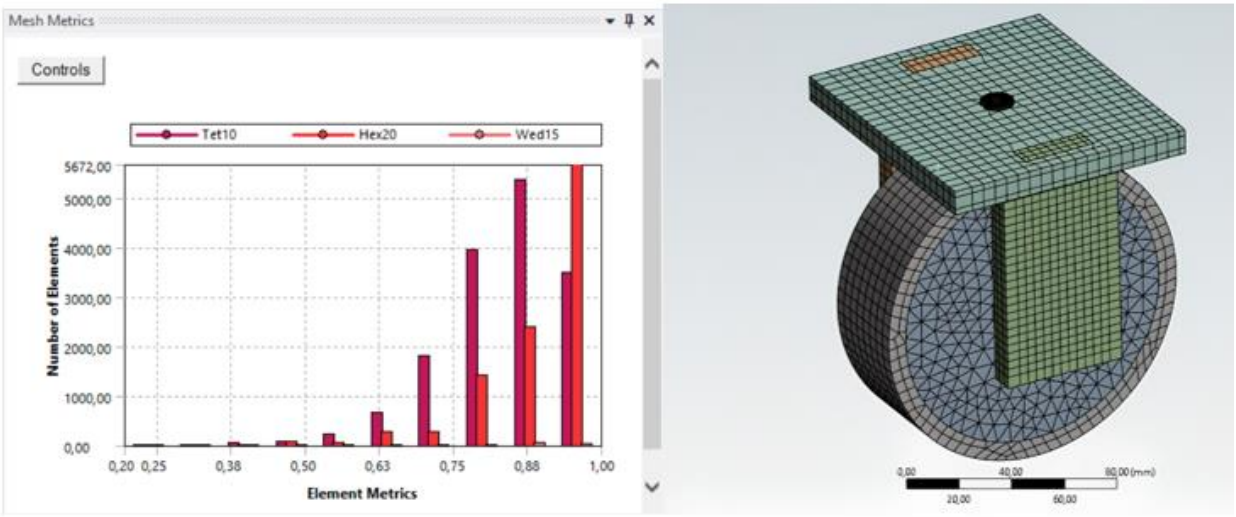

Figure 21. Wheel system mesh analysis

Upon examination of the mesh analysis results for the wheel system illustrated in Table 5, it becomes evident that the skewness and element quality values are calculated using 73,864 nodes and 25,743 elements following the implementation of the aforementioned improvements. Based on these calculations, the maximum skewness value is 0.92 and the average element quality value is 0.87. Because the values obtained were within the desired range, it is concluded that the mesh analysis is sufficient.

Table 5. Wheel system mesh analysis results

Number of Elements	Number of Nodes	Element Quality	Skewness
25743	73864	Max: 1 Avg: 0.87 Min: 0.19	Max: 0.92 Avg: 0.19 Min: $1.3x10^{-10}$

Mechanical analysis of the wheel mechanism was conducted under the assumption that the total weight of the vehicle with the maximum load (1800 N) would be borne by the wheels in the absence of friction.

The deformation and stress analyses of the wheel module as a function of the applied force are shown in Figures 22 and 23, respectively. As a result of these analyses, it can be seen that the total deformation value is between 0 and 0.04 mm, while the stress values are between 3.44×10-6 MPa and 75.37 MPa. Considering these results, it is observed that the wheel module is sufficiently durable to fulfill the desired task.

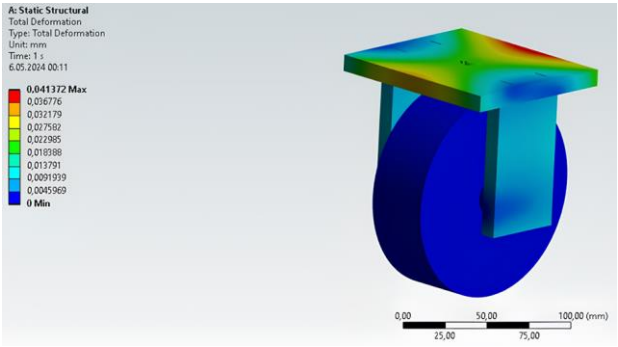

Figure 22. Wheel system deformation analysis

Figure 23. Wheel system stress analysis

3.4. Lift System

The vehicle's lifting system had dimensions of 400×360×323 mm. The upper and lower bases were constructed from aluminum alloys owing to their light weights. The scissors, cylinder, and pins were manufactured from stainless steel, owing to their durability. Analyses were conducted to assess whether these materials would also demonstrate the desired performance in practice. The results of the analysis are in accordance with the expected outcomes based on the calculations performed using the kinematic equations.

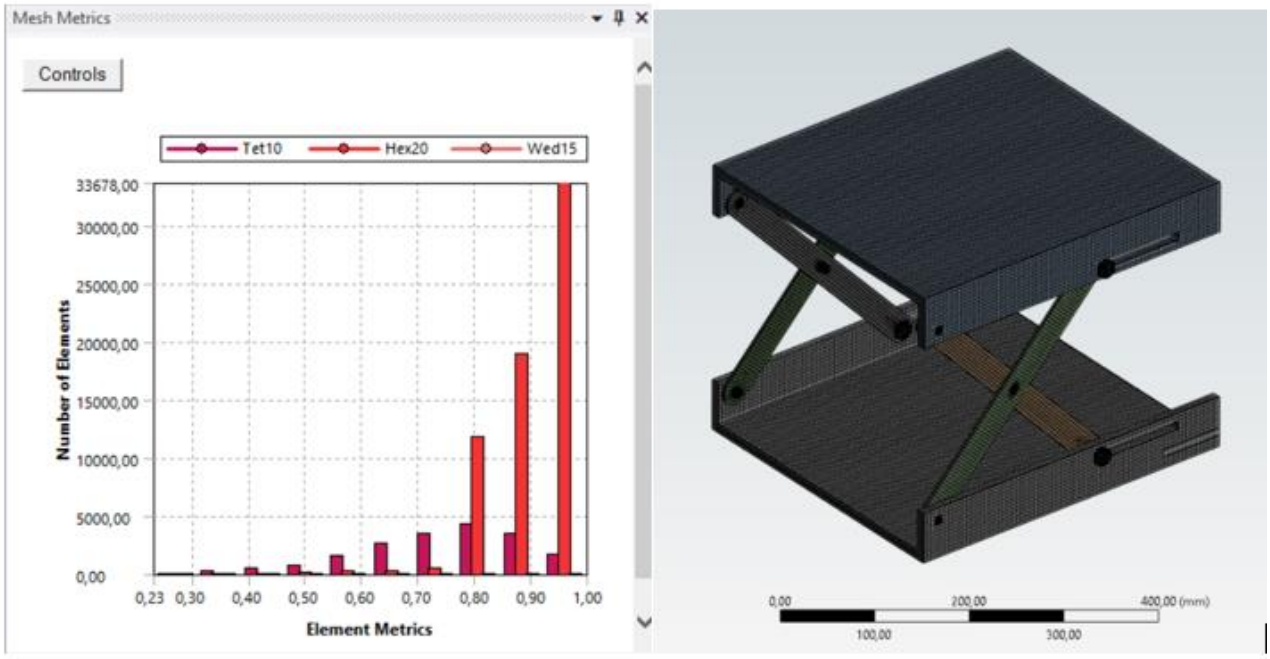

Figure 24. Lift system mesh analysis

Figure 25 illustrates the table of the mesh analysis for the element types, while Table 6 presents the results. As observed in Figure 24, tet10, hex20, and wed15 were utilized in the mesh analysis. As indicated in Table 6, there are 83944 elements and 381605 nodes. The average element quality value obtained from the table is 0.89, which indicates that the geometry is of a high quality and that the analysis can be conducted with confidence. The simplicity of the shape has resulted in the average skewness value coming out low at 0.098644. This indicates that the system is relatively balanced.

Table 6. Lift system mesh analysis results

Number of Elements	Number of Nodes	Element Quality	Skewness
83944	381605	Max: 1 Avg: 0.89 Min: 0.23	Max: 0.99 Avg: 0.0986 Min: $1.3x10^{-10}$

Figure 25 presents the results of the deformation analysis. The results indicate that the system is at a minimum deformation level, demonstrating high resistance to deformation. The maximum and minimum deformation values obtained are 0.65 mm and 0 mm. Figure 26 displays the stress analysis results against a 1250 N force applied to the system. The results indicate a maximum value of 58.76 MPa and a minimum value of 1.14×10^{-10} MPa. The choice of materials aluminum alloy and stainless steel confirms the system's outstanding resistance to stress and its capability to comfortably withstand loads up to 127.2 kg. Based on the analyses conducted, it can be concluded that the lift system designed is suitable for operational use.

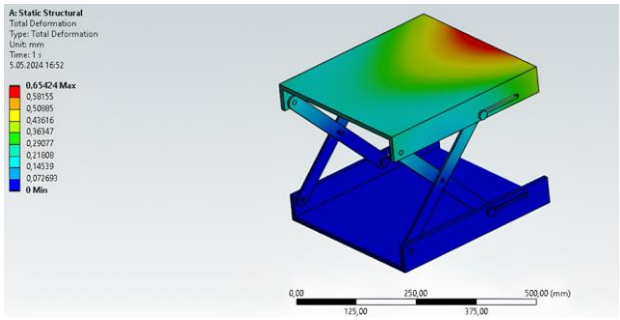

Figure 25. Lift system deformation analysis

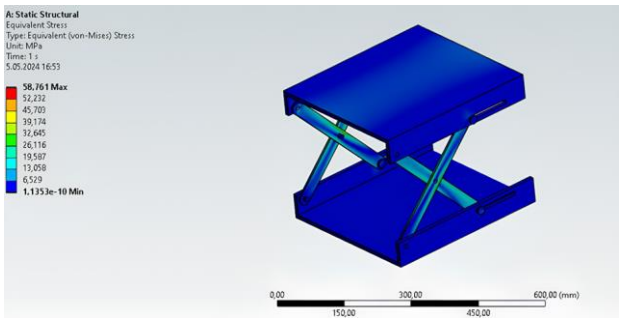

Figure 26. Lift system tension analysis

4. DISCUSSION AND CONCLUSION

This study focuses on the design, kinematic analysis, and mechanical durability of an autonomous mobile robot equipped with a scissor lift mechanism and a swerve drive system. The necessary electronic components for the vehicle's mobility and structural integrity have been identified, and kinematic formulas have been derived through theoretical calculations. The analyses conducted have confirmed that the vehicle can lift loads of the desired weight.

FEA was conducted utilizing Ansys to investigate the stress and deformation distributions of the vehicle under various loads, evaluating the vehicle's structural integrity

in simulated real-world conditions. A maximum deformation of 0.55 mm and a stress of 33.6 MPa were observed under a force of 325 N applied to the body. The chassis exhibited a maximum deformation of 0.1878 mm and a stress of 35.84 MPa under a load of 1300 N. The wheel mechanism demonstrated the capacity to support loads with a deformation of 0.04 mm and a stress of 75.37 MPa under a force of 1800 N. The lifting mechanism was analyzed with a force of 1250 N, resulting in a deformation of 0.65 mm and a stress of 58.76 MPa.

The analyses indicated that the vehicle, constructed of aluminum alloy and stainless steel, possesses the capacity to bear loads of up to 1250 N without significant deformation or stress. The quality of the mesh, skewness values, and element types (tet10, hex20 etc.) contributed to the accuracy and reliability of the analyses.

This study focuses on the avoidance system of the mobile robot, neglecting significant factors such as the control of the lever system and frictional forces. However, in practical applications, these omitted factors can substantially impact the vehicle's performance. Notably, temperature variations are critical to the long-term durability of the design. Thermal expansion at elevated temperatures or contraction at low temperatures can result in deformation and loss of precision in mechanical systems. Furthermore, particulate matter, prevalent in industrial environments, can increase frictional forces on wheel steering mechanisms, potentially leading to obstructions or wear. This may affect steering accuracy, particularly in independent wheel control systems. Additionally, while static load tests verify instantaneous structural durability, it is essential to consider that the vehicle will be subject to fatigue and wear effects during prolonged use. Repetitive loads can cause mechanical components to deteriorate over time, increasing the risk of failure. Moreover, the vibrations and sudden impacts that the mobile robot will experience in industrial applications can also negatively affect structural integrity. Considering these factors, it is evident that the elements disregarded in the design process can adversely impact the long-term performance and durability of the robot. Therefore, a more comprehensive analysis and testing against dynamic loads in conjunction with environmental factors could be conducted to obtain results more representative of real-world conditions.

Future research will encompass a more comprehensive analysis that incorporates the simulation of the lift system, as well as the effects of dynamic loads, friction, and dynamic behavior under varying operational conditions. Dynamic analysis—time-dependent assessments—will be conducted following the static analysis, as such analyses are more complex and time-consuming. However, they are essential for evaluating the system's performance under real-time external forces and changing speeds, ensuring reliable operation in real-world scenarios. Additionally, the development of path planning algorithms that enable the robot to navigate safely by sensing its environment is proposed. The application of deep learning methods and camera-based image processing techniques for object recognition will also be considered. Furthermore, techniques for effective mapping will be explored, enabling the robot to create a map of its environment and utilize it efficiently. Research will be conducted on SLAM (Simultaneous Localization and Mapping) algorithms, which allow robots to determine their positions while mapping unknown environments. The Gazebo simulation environment has been selected for these studies. The preference for Gazebo over CoppeliaSim is attributed to Gazebo's broader resources and the availability of numerous ready-made packages that can integrate seamlessly with ROS (Robot Operating System). This will facilitate more efficient and straightforward execution of tasks such as mapping, image processing, and simulation integration.

REFERENCES

[1] Haruna AI, Sankar R, Samaila A. Design and development of an instructional mobile robot for effective learning of material handling in mechanical workshops in universities. Mater Today Proc. 2023.

[2] Corke P. Robotics, Vision and Control: Fundamental Algorithms in MATLAB®. 1st ed. Berlin: Springer-Verlag; 2011.

[3] Tagliavini L, Colucci G, Botta A, Cavallone P, Baglieri L, Quaglia G, et al. Wheeled Mobile Robots: State of the Art Overview and Kinematic Comparison Among Three Omnidirectional Locomotion Strategies. J Intell Robot Syst. 2022;106(3).

[4] Raikwar S, Fehrmann J, Herlitzius T. Navigation and control development for a four-wheel-steered mobile orchard robot using model-based design. Comput Electron Agric. 2022; 202:105432.

[5] Yamaç Hİ, Yılmaz T. Mobil Robotlar için Yük Altındaki Davranış Analizinin İncelenmesi. Fırat Üniversitesi Mühendislik Bilimleri Dergisi. 2022;34(1):433-8.

[6] Roland Siegwart and Illah R. Nourbakhsh, Introduction to Autonomous Mobile Robots, 1st ed. Cambridge, Massachusetts: MIT Press; 2004.

[7] Demir C, Bozdemir M. Swedish tekerlekli mobil robot tasarımı ve 3b yazıcıyla imalatı, 4th International Congress On 3d Printing (Additive Manufacturıng) Technologies and Digital Industry, Antalya: 2019. p. 144-153.

[8] Huang H, Gao J. Backstepping and Novel Sliding Mode Trajectory Tracking Controller for Wheeled Mobile Robots. Mathematics. 2024;12(10):1458.

[9] Nikishkov GP. Introduction To The Finite Element Method. Japan: 2004 Lecture Notes. University of Aizu, Aizu-Wakamatsu 965-8580; 2004

[10] Baskoro CHAHB, Saputra HM, Mirdanies M, Susanti V, Radzi MF, Aziz RIA. An Autonomous Mobile Robot Platform for Medical Purpose. 2020 International Conference on Sustainable Energy Engineering and Application (ICSEEA). Tangerang: IEEE; 2020. p. 41-44.

[11] Yan SYW, Chamniprasart K, Phueakthong P, Pinrath N. Autonomous Mobile Robot for Material Handling in an Industrial Plant. The Annual

Conference on Engineering and Information Technology. Osaka: ACEAIT; 2023.
[12] Dhelika R, Hadi AF, Yusuf PA. Development of a Motorized Hospital Bed with Swerve Drive Modules for Holonomic Mobility. Applied Sciences. 2021;11(23):11356.
[13] Zhao Z, Xie P, Meng MQ-H. ODD: Omni Differential Drive for Simultaneous Reconfiguration and Omnidirectional Mobility of Wheeled Robots. arXiv preprint arXiv:2407.10127 (2024).
[14] Demir N, Sucuoglu HS, Bogrekci I, Demircioglu P. Structural & Dynamic Analyses and Simulation of Mobile Transportation Robot. Int. J. of 3D Printing Tech. Dig. Ind. 2021; 5(3): 587- 595.
[15] Prabhakaran S, Aravinth KT, Adhik N, Vikram R. Design and Analysis of Autonomous Mobile Robot. Nat. Volatiles & Essent. Oils. 2021; 8(5): 3020-3030.
[16] Koca YB, Gökçe B, Aslan Y. ROS/Gazebo Ortamında Tank Sürüş Özellikli Mobil Bir Robotun Similasyonu. Journal of Materials and Mechatronics: A (JournalMM). 202; 1(1), 29-41.
[17] Ağralı E, Çavaş M. V-REP Robotik Simülatör ile Robot Kol Simülasyonu. Fırat Üniversitesi Mühendislik Bilimleri Dergisi. 2020;32(2):435-44.
[18] Akin JE. Finite Element Analysis Concepts via SolidWorks. Rice University. Houston, Texas; 2009.
[19] Aksoy S. Makas Platformlu Mobil Robot Tasarımı ve Analizi [Bitirme Tezi]. Konya: Konya Teknik Üniversitesi Mühendislik ve Doğa Bilimleri Fakültesi; 2023.
[20] Madier D. An Introduction to the Fundamentals of Mesh Generation in Finite Element Analysis. FEA Academy; 2023
[21] Ansys. The Fundamentals of FEA Meshing for Structural Analysis. 2021 April 28 [cited 2024 September 28]. Available from: https://www.ansys.com/blog/fundamentals-of-fea-meshing-for-structural-analysis
[22] Cadsay. Ansys nedir?. [cited 2024 April 28]. Available from: https://cadsay.com/ansys-nedir
[23] Coppelia Robotics. CoppeliaSim. [cited 2024 April 27]. Available from: https://www.mathworks.com/products/connections/product_detail/coppeliasim.html
[24] Büyükarslan P. Spyder Nedir? Nasıl Kurulur?. [cited 2024 April 30]. Available from: https://www.sistemlinux.org/2018/05/spyder-nedir-nasil-kurulur.html
[25] Adar NG. Mobil İnsansı Robot Tasarımı İmalatı ve Kontrolü [Doktora Tezi]. Sakarya: Sakarya Üniversitesi Fen Bilimleri Enstitüsü; 2016.
[26] van der Velde P. Swerve drive introduction. 2022 December 4 [cited 2023 Jun 13]. Available from: https://www.petrikvandervelde.nl/posts/Swerve-drive-introduction
[27] Chiefdelphi, Whitepaper: Swerve Drive Skew and Second Order Kinematics. 2022 November [cited 2023 Jun 10]. Available from: https://www.chiefdelphi.com/t/whitepaper-swerve-drive-skew-and-second-order-kinematics/416964
[28] Gong Z, Nie Z, Liu Q, Liu XJ. Design and control of a multi-mobile-robot cooperative transport system based on a novel six degree-of-freedom connector. ISA Trans. 2023;139:606-20.
[29] Sukop M, Grytsiv M, Jánoš R, Semjon J. Simple Ultrasonic-Based Localization System for Mobile Robots. Applied Science. 2024;14(9):3625.
[30] Akyol S, Uçar A. Rp-Lidar ve Mobil Robot Kullanılarak Eş Zamanlı Konum Belirleme ve Haritalama. Fırat Üniversitesi Mühendislik Bilimleri Dergisi. 2019;31(1):137-43.
[31] Güngör O. Kaçak Elektrik Kullanımının GSM Aracılığıyla Takibi. EMO Bilimsel Dergi. 2015;4(8):29-34.
[32] Nalbantoğlu V, Seymen B. Ataletsel Seyrüsefer Sistemleri. Mühendis ve Makina. 2007;48(566):7-13.
[33] JR Callister WD, Rethwisch DG. Materials Science and Engineering: An Introduction. 10th ed. Hoboken, NJ: Wiley; 2018.
[34] FEATips. ANSYS Mesh Metrics Explained. 2022 November 21 [cited 2024 June 15]. Available from: https://featips.com/2022/11/21/ansys-mesh-metrics-explained/
[35] Simscale. Mesh Quality. 2024 July 30 [cited 2024 September 20]. Available from: https://www.simscale.com/docs/simulation-setup/meshing/mesh-quality/
[36] Bommes D, Lévy B, Pietroni N, Puppo E, Silva C, Tarini M, et al. Quad-Mesh Generation and Processing: A Survey. Computer Graphics Forum. 2013;32(6): 51-76.
[37] Motooka Y, Noguchi S, Igarashi H. Evaluation of Hexahedral Mesh Quality for Finite Element Method in Electromagnetics. Materials Science Forum. 2010;670:318–324.